ACS OMEGA

http://pubs.acs.org/journal/acsodf

Review

Ferroelectric Materials and Their Applications in Activation of Small Molecules

Weitong Ding,[⊥] Jing Lu,[⊥] Xiao Tang,* Liangzhi Kou,* and Lei Liu*

Cite This: *ACS Omega* 2023, 8, 6164−6174

Read Online

ACCESS | Metrics & More | Article Recommendations

ABSTRACT: The demand for renewable and environmentally friendly energy sources has attracted extensive research on high-performance catalysts. Ferroelectrics, a class of materials with switchable polarization, are unique and promising catalyst candidates due to the significant effects of polarization on surface chemistry and physics. The band bending at the ferroelectric/semiconductor interface induced by the polarization flip promotes charge separation and transfer, thereby enhancing the photocatalytic performance. More importantly, the reactants can be selectively adsorbed on the surface of ferroelectric materials depending on the polarization direction, which can effectively lift the basic limitations as imposed by Sabatier's principle on catalytic activity. This Review summarizes the latest developments of ferroelectric materials and introduces ferroelectric-related catalytic applications. The possible research directions of 2D ferroelectric materials in chemical catalysis are discussed at the end. The Review is expected to inspire extensive research interests from physical, chemical, and materials science communities.

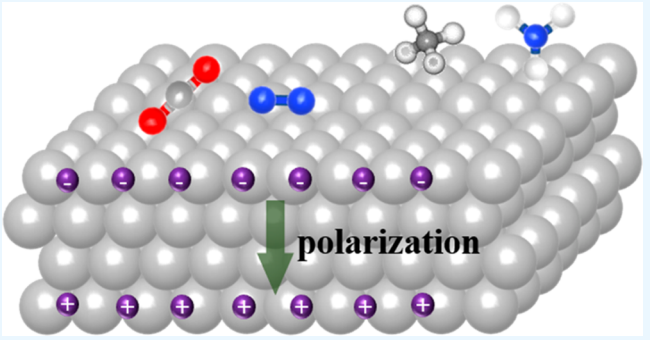

INTRODUCTION

With the rapid development of society, more and more energies are needed to meet the massive energy consumptions required for human life and activities; however, the increasing consumption of fossil fuels has led to serious environmental pollution. Hence, catalytic reduction technology has attracted extensive attention because of its ability to produce renewable chemical fuels,[1−5] for which looking for catalysts with high efficiency and selectivity is one of the key tasks. Recently, ferroelectric materials have been considered to be promising candidates for high-performance chemical reactions, since they are expected to overcome the limitations of the Sabatier principle. For example, ferroelectric $BiFeO_3$ can reduce the charge recombination rate of the $BiVO_4$ anode from 17 to 0.6 s^{-1} and increase the oxygen evolution rate of photoelectrochemical (PEC) devices by about 4.4 times.[6] This enhancement effect is mainly attributed to the spontaneous polarization of ferroelectric materials. The generated built-in electric field inside ferroelectric materials is beneficial to separate photogenerated electrons and holes. The charge imbalance induced by the field will be compensated by accumulating an equal amount of opposite charges on the surface by simple electronic reconstruction. Alternatively, electrons or holes are transferred to the opposite surfaces to compensate the charge imbalance[7−9] by atomic reconstruction, namely adsorption or desorption of certain atoms on the surface of the materials. In addition, the different electrostatic potential and electron distribution of ferroelectric materials will also lead to different surface chemical activity and redox reaction capabilities. The chemical properties of the catalyst surfaces can therefore be controlled via ferroelectric switching to improve the catalytic efficiency. Therefore, the application of ferroelectric materials in catalysts provides new opportunities for new catalysts with high performance.

Two-dimensional (2D) materials with atomic thickness show unique electronic,[10,11] optical,[12,13] mechanical,[14] and thermal[15] properties, which have not been found in bulk counterparts.[16] It provides new ideas for the research of 2D ferroelectric materials. Generally, 2D materials consist of one or several atomic layers, and due to the inherent size and surface effects their ferroelectric properties are significantly different from those of traditional bulk counterparts. The depolarization field is significantly enhanced at 2D limits. Meanwhile, due to the reduction in the size of the material in the direction perpendicular to the plane, the surface of the 2D ferroelectric material has a richer morphology and active

Received: November 5, 2022
Accepted: January 11, 2023
Published: February 9, 2023

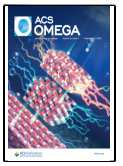

https://doi.org/10.1021/acsomega.2c06828
ACS Omega 2023, 8, 6164−6174

chemical environment, and its microstructure is easier to control compared with bulk materials. For example, polar nanoregions (PNR) in $SrTiO_3$ thin films with a less than 3 unit cells (3-u.c.) thickness can be easily polarized.[17] The research of Kolpak and Wang showed that the special surface of 2D ferroelectric materials can effectively compensate the depolarization field.[18,19] Moreover, van der Waals-type 2D ferroelectric materials have good durability against large strains. Unlike the surface of other 2D ferroelectrics, van der Waals-type 2D materials have a more stable surface structure, which may help maintain ferroelectric polarization,[20] as in MoS_2 and In_2Se_3.[21,22] Up to date, a series of 2D ferroelectric materials have been theoretically predicted and experimentally verified, such as MXenes, group IV monosulfur compounds, III_2-VI_3 compounds, transition metal dichalcogenides, and transition metal phosphochalcogenides. This Review will start with a brief introduction of traditional ferroelectric materials, followed by current experimental synthesis and theoretical prediction of 2D ferroelectric materials, and then their applications in catalysis.

RESULTS AND DISCUSSION

Traditional Ferroelectric Materials. Ferroelectric materials refer to the materials that have two or more spontaneous polarization directions at certain temperatures, and such spontaneous polarization can be flipped under an external electric field.[23,24] The essence of spontaneous polarization is the ion offset caused by the asymmetry of the crystal structure. Generally, the polarization of the materials depends on the external electric fields. Under the external electric field, the ion offset could be changed, which is called polarization inversion (Figure 1a). Therefore, ferroelectric materials show several

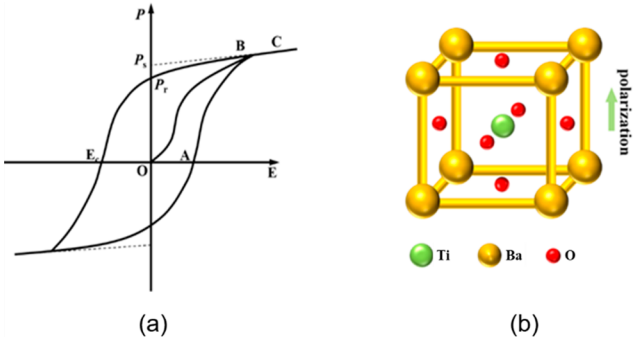

Figure 1. (a) Ferroelectric polarization curve. (b) Schematic diagram of atomic structures of perovskite ferroelectric materials.

important characteristics, such as dielectric effect, piezoelectricity, pyroelectricity, ferroelectricity, electro-optic effect, and acousto-optic effect, which could be used to fabricate ferroelectric memory, infrared detectors, and capacitive devices.[25] Traditional ferroelectric materials can be divided into five types: perovskite, pyrochlore, tungsten bronze, lithium niobate, and bismuth-containing layered structures. Among them, the ferroelectric material with the perovskite structure is the most studied one. The following contents will briefly introduce this type of structure, by taking the $BaTiO_3$ material as a representative example (Figure 1b).

With the change of temperature, $BaTiO_3$ undergoes a phase transition: the cubic phase to the tetragonal phase (~130 °C), to the orthorhombic phase (~0 °C), and to the rhombohedral phase (~−90 °C).[26−29] At room temperature, the ferroelectric polarization is robust along the *c*-axis. When the temperature is higher than the Curie temperature (~130 °C), $BaTiO_3$ is a cubic crystal system, in which Ti^{4+} locates in the center of the octahedron with the same probability of approaching the surrounding six O; thus, it does not have spontaneous polarization. $BaTiO_3$ becomes a tetragonal structure below 130 °C, and Ba^{2+} shifts from the original equilibrium position along the (001) direction, while the Ti^{4+} is still located in the center of the tetrahedron with reduced thermal energy. Some Ba^{2+} move toward certain O (such as O in the *c*-axis direction), resulting in spontaneous polarization. When the crystal exhibits spontaneous polarization, a layer of positive and negative charges will be created, and an electric field opposite to the polarization direction is generated between the positive and negative charges, which is called depolarization. The electric field, which exists in the crystal, will increase the internal electrostatic energy and render the structure unstable. In order to eliminate the effect of the built-in electric field, multiple regions with different polarization orientation are usually formed in the materials, which are the so-called ferroelectric domains. Moreover, the internal electric field can be offset by the reconstruction of electrons or atoms, leading to the different catalytic ability in the opposite surfaces of ferroelectric materials.

The size and fatigue effects of ferroelectric materials are important reasons to restrict their applications in electronic devices and chemical catalysis, since stable polarization can only exist in ferroelectric thin films with the critical thickness of about tens of nanometers.[30] Ferroelectricity of traditional perovskite oxides will be significantly weakened or even disappear when they are thinner than several unit cells, such as 1.2 nm for $PbTiO_3$, 2.4 nm for $BaTiO_3$, and 3.0 nm for $BiFeO_3$.[31,32] However, there are several exceptions; for example, in the ultrathin strain-free $SrTiO_3$ film, ferroelectricity can even be enhanced in low dimensions.[33] For recently emerging 2D ferroelectric materials, there are already several comprehensive reviews.[34−36] Here, we only focus on several heavily studied 2D examples and their structural properties in the next section.

2D Ferroelectric Materials. *MXenes.* In 2011, Naguib et al. stripped Ti_3C_2 at room temperature to obtain Ti_3C_2 nanostructures, which opened a new area for 2D materials.[37] The general expression of 2D MXenes is $M_{n+1}X_n$, where M = an early transition metal and X = C or N, n = 1, 2, 3. This type of 2D material is usually made from a huge family of the MAX phase (where A = an element from group 13 or 14 of the periodic table).[38−40] More than 30 different MXenes have been synthesized and predicted so far.[37] Researchers have found that MXenes have a variety of chemical properties, which makes them widely used. Among them, energy storage is the most studied application, in addition to water purification,[41] catalysis,[42−45] and reinforced composite materials.[46] Since the strengths of the M−A bonds and M−X bonds are different, MXenes are often synthesized by controlling the temperature and using corrosion methods.[38] Due to the different reagents used in the corrosion process, the surfaces of MXenes could have different functional groups, such as O, OH, F, Cl, and S, to modify electronic properties of MXenes. The surfaces of traditional MXenes are often highly reactive, which provides the possibility to induce ferroelectricity.[38,47] For example, Chandrasekaran et al. used first-principle calculations to obtain the polarization value of Sc_2CO_2,

https://doi.org/10.1021/acsomega.2c06828
ACS Omega 2023, 8, 6164−6174

which is 1.60 μC/cm^2.[48] As shown in Figure 2, Zhang et al. investigated three types of ferroelectric MXene phases, i.e.,

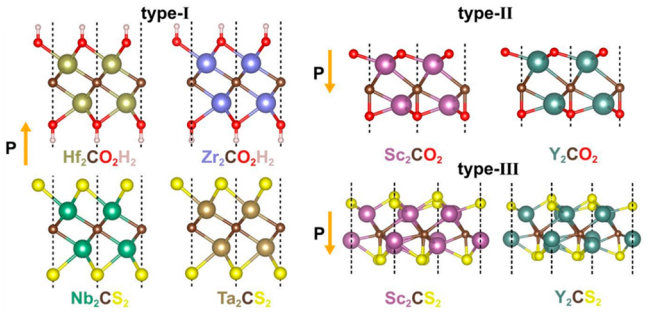

Figure 2. Ferroelectric MXenes. The orange arrows indicate the direction of out-of-plane polarization. Reproduced with permission from ref 49. Copyright 2020 Royal Society of Chemistry.

type I: Nb_2CS_2 and Ta_2CS_2; type II: Sc_2 CO_2 and Y_2CO_2; type III: Sc_2CS_2 and Y_2CS_2, by using high-throughput searches and DFT calculations,[49] and they found that these structures could exhibit robust ferroelectricity in both out-of-plane and in-plane directions.

Group IV Monosulfur Compounds. The general expression of group IV monosulfur compounds is MX (M = Sn or Ge, X = Se or S), which has the same orthogonal structure as black phosphorus.[50−53] Recently, the studies showed that group IV monosulfide monolayers are multiferroic with large ferroelectric and ferroelastic coupling.[54] As shown in Figure 3a, the

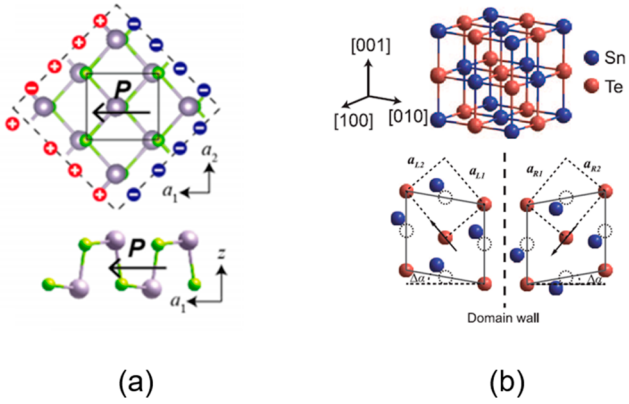

Figure 3. (a) Lattice structure of the SnSe monolayer. The arrow in the figure indicates the direction of ferroelectric polarization. Reproduced from ref 51. Copyright 2020 American Chemical Society. (b) Schematics of the SnTe crystal structure and the lattice distortion and atom displacement in the ferroelectric phase. Reproduced with permission from ref 55. Copyright 2016 American Association for the Advancement of Science.

lone pair electrons of Ge/Sn ions may make their structure distorted, resulting in in-plane switchable ferroelectricity. Moreover, their Curie temperature was predicted to be 326−6400 K, which is an unimaginable value in 2D materials.[54] In 2016, Chang et al. reported the polarization performance of ultrathin tin telluride (SnTe) at the liquid helium temperature.[55] Using scanning tunneling microscopy (STM) and scanning tunneling spectroscopy (STS), stable fringe regions, lattice distortion, band bending, and electrical polarization operations were observed in SnTe with a thickness of 1 u.c. The polarization characteristic of SnTe is considered to be caused by the change of the ideal square formed by Te atoms into a parallelogram, as shown in Figure 3b. Moreover, 2−4 u.c. SnTe films also showed strong ferroelectricity at room temperature.[56] Inspired by the study of 2D ferroelectric SnTe, Wan et al. predicted possible ferroelectric phases in group IV tellurides.[56−58]

III_2−VI_3 Compounds. These compounds are stable single-layer 2D ferroelectric materials based on III−VI compounds, with the general expression being A_2B_3, where A = Al, Ga, In; B = S, Se, Te. As early as 1990, Abrahams proposed that In_2Se_3 might be a ferroelectric based on structural analysis.[59] The single-layer structure of In_2Se_3 consists of Se and In layers alternately arranged by covalent bonds, and the arrangement sequence is Se−In−Se−In−Se. The origin of its ferroelectricity is believed to be the unequal interlayer spacing between the Se layer and two adjacent In layers.[60] In_2Se_3 usually has five known forms (e.g., α, β, γ, δ, and κ), among which the α phase is considered to be the most stable layered structure at room temperature (Figure 4).[61] Zhou et al. reported that the

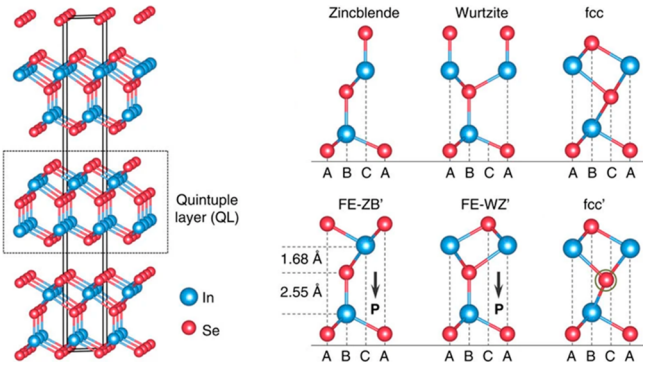

Figure 4. Three-dimensional crystal structure of layered In_2Se_3 (left) and side views of several representative structures of one QL In_2Se_3 (right). Reproduced with permission from ref 61. Copyright 2017 Springer Nature.

multilayer α-In_2Se_3 with a film thickness of 10 nm has piezoelectric and ferroelectric properties.[62] They observed ferroelectric domains through piezoelectric response force microscopy (PFM), with obvious phase contrast and domain wall boundaries. Xiao et al. reported the intrinsic ferroelectric properties in thin In_2Se_3 crystals with an atomic layer thickness of less than 3 nm and verified the polarization locking mechanism by second harmonic generation (SHG) spectroscopy measurement and PFM.[63] Ding et al. systematically investigated a series of A_2B_3 materials by DFT calculations,[61] and the results showed that the ferroelectric phases FE-ZB and FE-WZ are also the ground states of Al_2S_3, Al_2Se_3, Al_2Te_3, Ga_2S_3, Ga_2Se_3, Ga_2Te_3, In_2S_3, and In_2Te_3. In short, this type of 2D ferroelectric material has inherent out-of-plane and in-plane electric polarization. With the aid of an appropriate out-of-plane or in-plane electric field, these electric polarizations can be converted through a dynamic approach.

Transition Metal Dichalcogenides. Transition metal disulfides can reduce their atomic structures to the nanometer scale and do not require lattice reconstructions.[64] Their structures are noncentrosymmetric, which provides a basis for the existence of ferroelectricity.[65] In 2014, piezoelectricity was found in MoS_2 monolayers, yet this characteristic only exists in odd-numbered layers.[66,67] In the same year, 1T single-layer

https://doi.org/10.1021/acsomega.2c06828
ACS Omega 2023, 8, 6164−6174

MoS_2 (d1T-MoS_2) was predicted as a ferroelectric material. The two sulfur lattice planes are arranged in a way such that each Mo site becomes the center of inversion, making 1T-MoS_2 a promising candidate for ferroelectricity (Figure 5a and b).[68] Similar calculations were extended to some other 1T MX_2 (M = Mo, W; X = S, Se, Te) with twisted octahedral coordination structures (t-MX_2), as shown in Figure 5c.[69] They found that all t-MX_2 monolayers with d2 metal ions show spontaneous dielectric polarization, which makes TMDs materials promising for 2D ferroelectric materials. In 2018, the study of topological semimetal tungsten ditelluride (WTe_2) once again enriched this type of ferroelectrics,[69] and the authors proposed that the polarization of WTe_2 is caused by the relative movement of the electron cloud related to the ion nucleus.

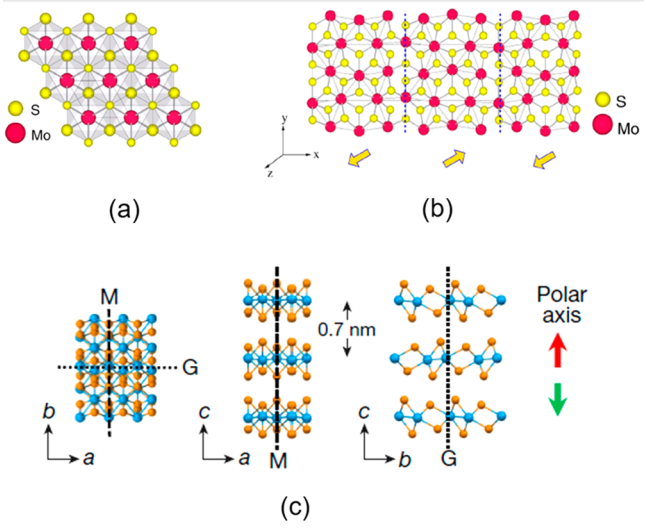

Figure 5. (a). Top view of the structure of a monolayer of MoS_2 in c1T polytypical form with octahedral coordination of Mo atoms. (b) Structure of the domain wall (blue dashed line) between up- and down-polarized states of d1T. Reproduced with permission from ref 68. Copyright 2017 American Physical Society. (c) Structure of three-dimensional 1T′-WTe2, showing the mirror plane (M; dashed), glide plane (G; dotted), and polar c-axis (red arrow, up; green arrow, down). W atoms are blue; Te atoms are orange. Reproduced with permission from ref 69. Copyright 2018 Springer Nature.

Transition Metal Phosphochalcogenides (TMPs). TMPs are a large class of van der Waals layered solids, and their general expression is ABP_2X_6, where A or B is a combination of monovalent/trivalent or divalent/divalent and X is a chalcogenide, including S, Se, Te, etc.[70,71] One of the important characteristics is that the van der Waals forces between the layers are very weak; hence, a thin film can be easily peeled from the single crystal. The most representative example is $CuInP_2S_6$, which contains a sulfur skeleton, and the triangular patterns of Cu, In, and P are filled with octahedral voids (Figure 6a and b). This special structure makes it possible to have ferroelectric or antiferroelectric characteristics.[72] In 1994, the paraelectric−ferroelectric phase transition of $CuInP_2S_6$ was observed experimentally at 315 K.[73] Later, Belianinov et al. reported that the thickness of the ferroelectric $CuInP_2S_6$ film can be achieved as low as 50 nm,[74] which provides an opportunity to obtain ferroelectric $CuInP_2S_6$ at the nanometer scale. After that, Liu et al. reported the room temperature ferroelectricity of ultrathin $CuInP_2S_6$ (~4 nm),

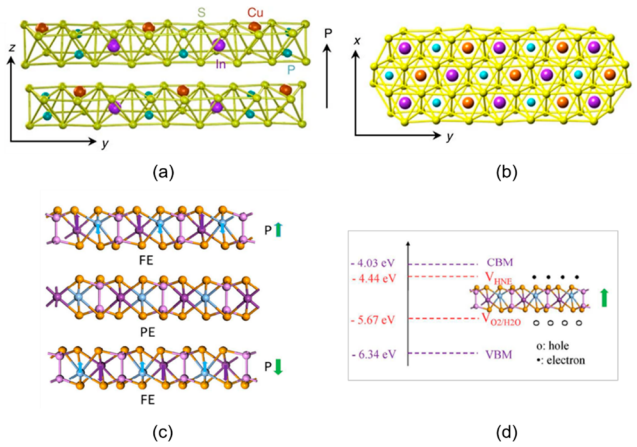

Figure 6. Side view (a) and top view (b) for the crystal structure of $CuInP_2S_6$ with a vdW gap between the layers. The polarization direction is indicated by the arrow. Reproduced with permission from ref 75. Copyright 2016 Springer Nature. (c) Side view of two distorted ferroelectric phases with different polarization directions (top and bottom) and a high-symmetry paraelectric phase (center). (d) Band edge of single-layer $AgBiP_2Se_6$. Reproduced with permission from ref 78. Copyright 2017 Royal Society of Chemistry.

and the transition temperature is 320 K.[75] This spontaneous polarization is caused by the moving of the Cu sublattice from center symmetry to the In sublattice. The antialignment dipole greatly reduces the depolarization field inside $CuInP_2S_6$, so that stable polarization is shown at an ultrathin thickness.[76,77] In 2017, Xu et al. used first-principles to design a new TMTP material, $AgBiP_2Se_6$, as shown in Figure 6c. Among them, the deviation of the Ag^+ and Bi^{3+} causes the adjacent unit cells to have different polarizations in the same direction, thus forming a stable ferroelectric phase with a polarization value of about 0.2 $\mu C/cm^2$.[78] Figure 6d is the band edge of single-layer $AgBiP_2Se_6$ calculated by the HSE method, and the results show that the valence band minimum (VBM) of $AgBiP_2Se_6$ is 0.41 eV higher than the oxidation potential of water, while the conduction band maximum (CBM) is 0.67 eV lower than the hydrogen reduction potential. Therefore, single-layer $AgBiP_2Se_6$ exhibits the ability of a water-splitting catalyst.

Application of Ferroelectric Materials in Catalysis. Catalysis reaction involves complex reaction processes, which are often affected by several factors. For example: the binding strength between the adsorbate and the reaction surface, the electron transfer between the catalyst and the reactant, and the separation and recombination ability of photogenerated charges should also be considered in photocatalysis. Ferroelectric materials have also been shown to play a variety of promoting roles in catalytic reactions, in particular, activation or conversion of small energy-related molecules, which will be summarized in the next sections.

Gas Adsorption. Previous studies have known that ferroelectricity affects physical and chemical properties of the material's surface, which may enhance their interactions with gas molecules.[79] In 1952, Parravano observed that the CO oxidation rate of sodium niobate and potassium niobate near the Curie temperature was abnormal,[80] which opens up a new direction for the application of ferroelectric materials in chemistry. In 2006, Ramos-Moore et al. used the temperature-programmed desorption method (TPD) to study the CO_2 desorption energy of $KNbO_3$ at different temperatures.[81] Figure 7a and b shows the CO_2 desorption curves of $KNbO_3$

https://doi.org/10.1021/acsomega.2c06828
ACS Omega 2023, 8, 6164−6174

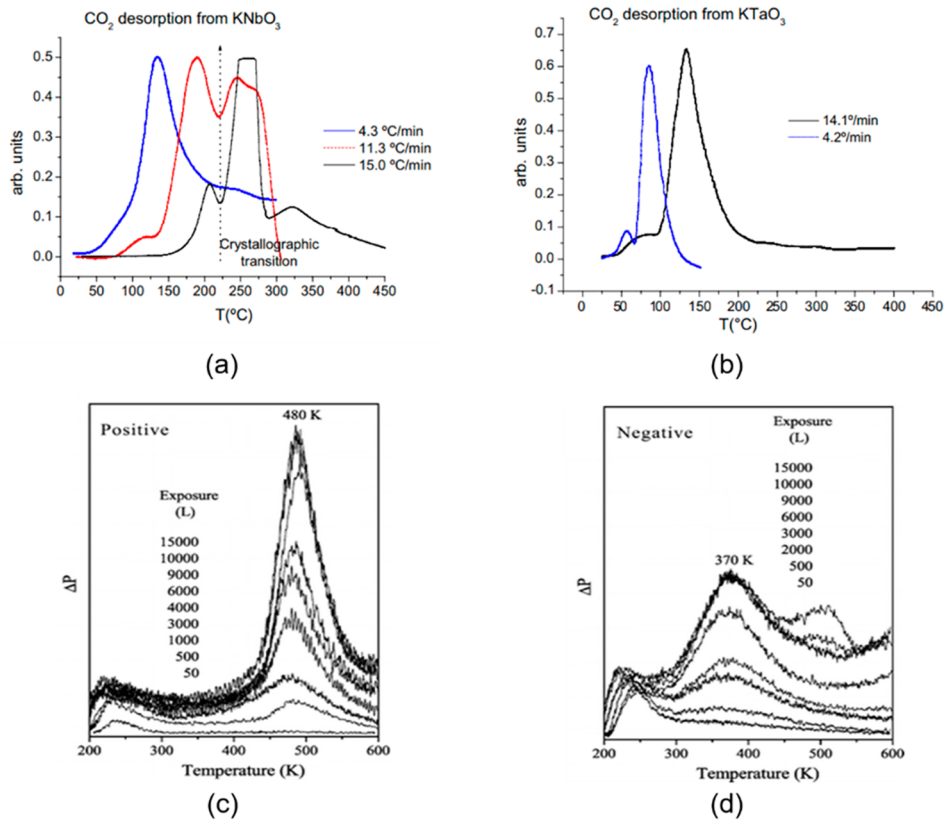

Figure 7. (a) Carbon dioxide desorption curves for powder of $KNbO_3$ at three different heating rates. (b) Carbon dioxide desorption curves for powder of $KTaO_3$ at two different heating rates. Reproduced with permission from ref 81. Copyright 2006 Elsevier. TPD traces for 2-propanol on positively (c) and negatively (d) poled $LiNbO_3$(0001) surfaces. Reproduced from ref 82. Copyright 2007 American Chemical Society.

powder with three different heating rates. It can be found that there are two peaks in the figure, but there is only one peak in $KTaO_3$. Interestingly, the position of the second peak is somehow independent of the heating rates, which is always near the phase transition temperature. The authors concluded that the appearance of the second desorption peak (580 K, after the phase transition temperature of 433 K) is related to the ferroelectric phase transition of $KNbO_3$, and CO_2 is adsorbed at the edge of the materials. In 2007, Yun et al. used the TPD method to study the adsorption properties of $LiNbO_3$ to polar and nonpolar molecules (two polar molecules, acetic acid and 2-propanol, and one nonpolar molecule, dodecane).[79,82] The results show that the adsorption and desorption temperature of the polar molecule acetic acid on the positive electrode surface of $LiNbO_3$ is about 101 K higher than that on the negative electrode surface (Figure 7c and d), while the nonpolar molecule is not affected by the polarized surface. With the same technique of TPD, Zhao et al.[83] investigated the polarization-dependent adsorption coefficient of ethanol on $BaTiO_3$, and the results show that ferroelectric materials not only change the number of active sites but also affect chemical reactions at the surface. Based on the experiments, the authors proposed a "precursor-mediated" mechanism; that is, ethanol first exists on the surface via physical adsorption, and when it encounters a defect site, it may react with surfaces and become chemical adsorption. On the other hand, DFT calculations showed that the chemisorption energies of a series of small molecules on the Pt(100)/$PbTiO_3$ surface could be dramatically changed by reorienting the polarization direction of the substrate.[84]

Based on the DFT calculations, Kakekhani et al.[85] studied the influence of external fields on the chemical properties of the surface of ferroelectric materials, $PbTiO_3$ (PTO), and the authors demonstrated that the surface could be periodically alternated between oxidizing, inert, and reducing behavior under cyclic polarization conditions.[7,86,87] Subsequently, they applied this knowledge to design catalytic cycles for several industrially important reactions. The results show that on the negatively polarized surface of PTO, SO_2 will get O atoms from the surface of PTO to generate SO_3. The studies of NO, NO_2, N_2, and O_2 on the polar surface show that polarization could be used as a switch to control their binding energies, and the alternation of positive and negative polarity could even overcome the problem of O inhibition for the direct decomposition of NO_x. The only limitation is that NO_x decomposition will not occur on a low PTO cover layer ($\leq$0.25 monolayer), which might be achieved via 2D ferroelectric materials.[7] Concerning the direct partial oxidation of CH_4 to CH_3OH, the authors found that the reaction prefers to occur on the negatively poled oxidizing surface, of which the energy barrier is ca. 1:1 eV, and the binding energy of CH_3OH is almost negligible.

Recently, by DFT calculations Tang et al. showed that the reversible polarization transition of the 2D ferroelectric-In_2Se_3 monolayer can effectively regulate the adsorption energies, electron transfer, and magnetic moment of the adsorbed metal porphyrazine (MPz) molecules.[88] The electrostatic potential difference between MPz molecules and In_2Se_3 monolayers illustrates that the unique behavior of adsorption energies and electron transfer, and the occupancy changes of d orbitals at

https://doi.org/10.1021/acsomega.2c06828
ACS Omega 2023, 8, 6164−6174

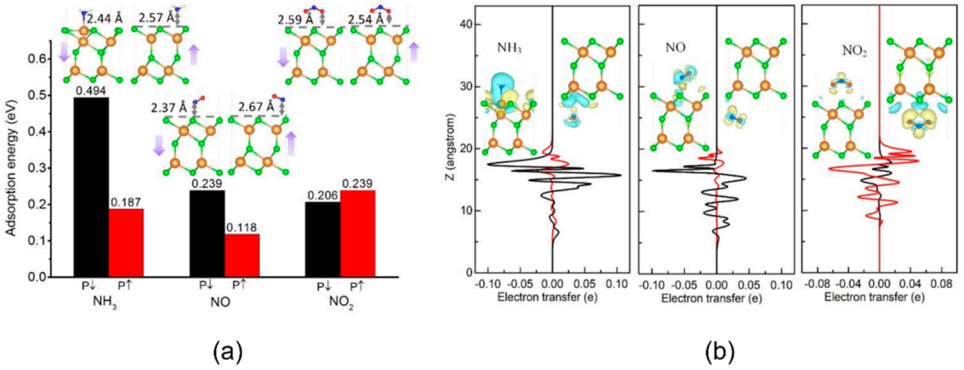

Figure 8. Adsorption energies (a) and electron transfer of NH_3, NO, and NO_2 on the In_2Se_3 monolayer (b). Reproduced with permission from ref 89. Copyright 2020 Royal Society of Chemistry.

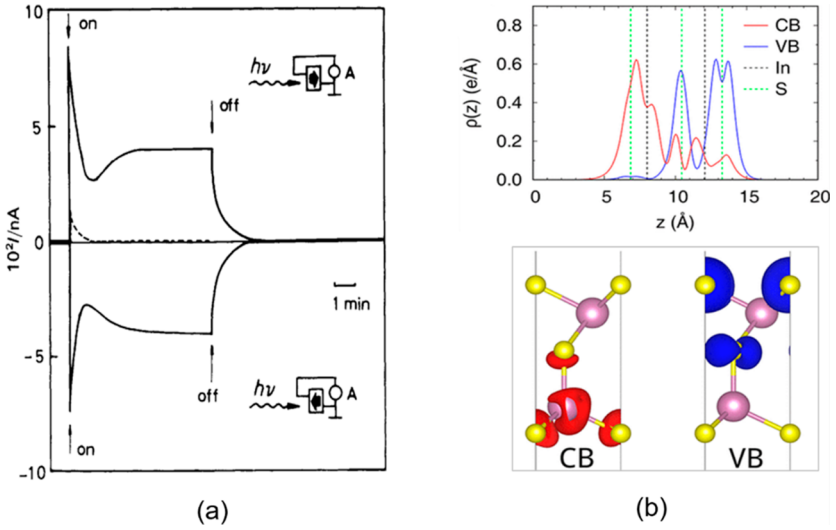

Figure 9. (a) Photoresponse of PKN (x = 0.006). Reproduced with permission from ref 93. Copyright 1990 Royal Society of Chemistry. (b) Distributions of VB and CB along the vertical direction (z-axis) for In_2S_3 monolayers (upper panel) and spatial distribution of CB and VB (lower panel). Reproduced from ref 95. Copyright 2018 American Chemical Society.

different polarizations are due to the magnetic ferroelectric tuning. At the same time, their research on the adsorption of a series of gas molecules (e.g., NH_3, NO, and NO_2) on the In_2Se_3 monolayer shows that there is an obvious polarization-dependent gas molecule adsorption behavior on the surface of the ferroelectric In_2Se_3 monolayer, which can achieve reversible gas adsorption and release controlled by the ferroelectric switch (Figure 8).[89] Later, the same procedure has been employed to control the adsorption behavior of O_2, CO, and H_2O on the Fe/Mn-doped graphene by taking In_2Se_3 as the substrate.[90] The above-mentioned phenomena are basically originated from the synergistic effect of different electrostatic potentials and electrons, which is caused by the band arrangement between the molecular orbitals of the gas front and the edge states of the baseband.[89] As a summary, the controllable ferroelectric adsorption behavior and molecular multiferroic characteristics could be widely used in gas adsorption.[83]

Catalysis. In photocatalytic reactions, polarization can well separate light-induced charge carriers to improve photocatalytic efficiency. For example, the recombination of photogenerated carriers and the reverse reaction of intermediate species are the main factors that limit the efficiency of water photolysis catalysts.[91] Ferroelectric materials have high surface energy and affect the electrical properties of the generated charge carriers, and the spatial selectivity of their surface may promote photocatalysis. It is known that the mechanism of the spatial selectivity of ferroelectric materials is due to spontaneous polarization, which can bend energy bands of crystals, thereby causing photogenerated electrons and holes to move in opposite directions, promoting the separation of holes and electrons.[92] In fact, a series of studies on the application of ferroelectric materials to photocatalysis have been carried out, as summarized in a review by Kakekhani.[86] Almost 30 years ago, Inoue et al.[93] studied the photoassisted water splitting on lead zirconate titanate (PZT) ceramics, with a focus on the effects of potassium addition on the photoelectric performance of hydrogen production from water. As shown in Figure 9a, when $Pb_{1-x}K_xNb_{20}$ (PKN) has polarization, it not only shows a large transient pyroelectric current, but also the subsequent current significant decays to almost zero. Recently, 2D ferroelectric materials have started to attract more attention in the vein of photoassisted water splitting.[94] A representative example was shown by Jin et al.[95] in which the authors investigated the potential feasibility of a series of 2D M_2X_3 (M = Al, Ga, In; X = S, Se, Te) materials for photocatalytic water splitting by using first-principles calculations (Figure 9b). The results show that all candidates are

https://doi.org/10.1021/acsomega.2c06828
ACS Omega 2023, 8, 6164−6174

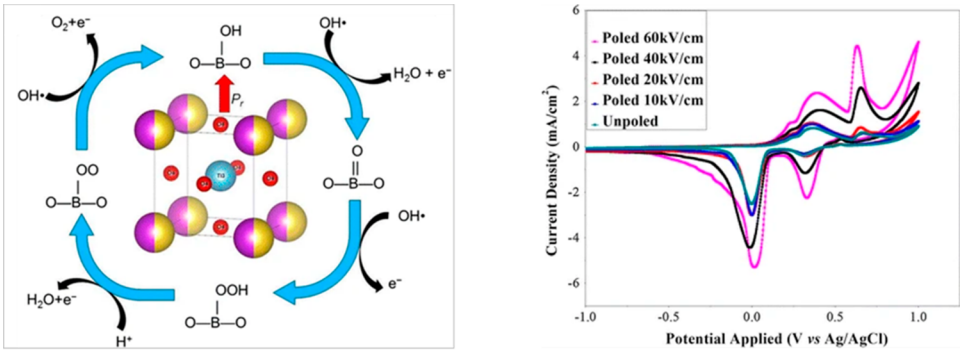

Figure 10. (a) Proposed OER mechanism for BNT ferroelectric catalysts. (b) Cyclic voltammograms of poled and unpoled BNT pellet electrodes in 0.1 M KOH at a scan rate of 100 mV/s. Reproduced with permission from ref 100. Copyright 2017 Springer Nature.

verified to be suitable for water splitting, of which the predicted solar-to-hydrogen efficiencies of Al_2Te_3, Ga_2Se_3, Ga_2Te_3, In_2S_3, In_2Se_3, and In_2Te_3 are larger than 10%. In particular, In_2Te_3 shows a supersizing high solar-to-hydrogen efficiency of 32.1%.

Another widely studied application of ferroelectric materials as photocatalysts is the reduction of Ag^+ to Ag. In 2001, Giocondi et al. irradiated $BaTiO_3$ with ultraviolet light in an aqueous solution containing dissolved Pb^{2+} or Ag^+ and found that Ag^+ reduction occurred on the positively polarized surface, while more Pb^{2+} oxidation occurred on the negatively polarized surface.[96] Later, Bhardwaj et al.[97] studied effects of Sr doping on the catalytic performance of $BaTiO_3$ and found that in $Ba_{1-x}Sr_xTiO_3$, the reduction effect on Ag^+ is the largest when x = 0.26. Subsequently, Schultz et al.[98] analyzed in detail the effects of crystal and domain orientation on the photochemical reduction of Ag on $BiFeO_3$. They found that $BiFeO_3$ is beneficial to the reduction of Ag^+, and this phenomenon corresponds to the ferroelectric domain structure. Moreover, they calculated the energy band diagrams of bulk $BiFeO_3$, and the results show that when the polarized surface comes into contact with the solution, the energy band will bend.

In electrocatalysis, the interactions between the reactant and the catalyst could be also affected by the polarization.[99] In 2018, Kushwaha et al.[100] investigated the effect of ferroelectric $Bi_{0.5}Na_{0.5}TiO_3$ (BNT) with different polarization values on the electrocatalytic oxygen evolution reaction (OER) (Figure 10). They found that iron polarization can be used to adjust the OER activity of BNT, which has a certain relationship with the built-in electric field generated by the polarization in BNT. The reason for this phenomenon is similar to that for photocatalysis: that is, the increase of iron polarization causes the energy band of the negative electrode surface to bend upward, while the energy band of the positive electrode surface bends downward. The latter helps to effectively transfer the generated charge from the surface of the catalyst to the electrolyte, thereby promoting the redox reaction. Moreover, Li et al.[101] studied the influence of layered ferroelectric oxides with different Co doping concentrations on the OER reaction. The results show that with the increase of Co content, more oxygen is absorbed on the surface. The OER performance of the pure cobalt-based oxide is 100 times higher than that of the pure iron-based oxide, which exceeds the precious metal benchmark IrO_2 catalyst. Similarly, iron polarization helps to reduce the overpotential by 70 mV for the OER reaction on the $Bi_5CoTi_3O_{15}$ (BCTO) composite catalyst, thereby providing a current density of 10 mA cm^{-2}.[102]

Moreover, the application of ferroelectric materials as electrocatalysts has been carried out in a series of small-molecule activation. Taking In_2Se_3 as an example, Kim[103] constructed a catalytic system with In_2Se_3 on top of the hexagonal close-packed (HCP) Co metal slab and investigated its hydrogen evolution reaction (HER) performance via ab initio calculations. The author found that the reversible polarization switching of In_2Se_3 can turn the HER activity of the heterostructure ON and OFF. Meanwhile, Kan et al.[104] studied a Pt single-atom catalyst by taking the ferroelectric monolayer In_2Se_3 as the substrate, and the results show that Pt atom strongly interacts with In_2Se_3 and has a negative clustering energy. Importantly, the Pt/In_2Se_3 catalyst shows extremely high activity for CO oxidation, which could be even regulated by the ferroelectric switch of monolayer In_2Se_3. Very recently, Kou and his co-workers[105] examined a series of catalytic systems, TM@In_2Se_3 (TM = Ni, Pd, Rh, Nb, and Re), for the electrochemical reduction of CO_2. Through extensive ab initio calculations, the authors identified the Rh@In_2Se_3 catalyst as a highly efficient electrochemical catalyst with a fairly low limiting potential (<0.5 V). Interestingly, they found that Re@In_2Se_3 and Nb@In_2Se_3 catalysts can realize selective generation of desired products via polarization switching.

CONCLUSION

This Review mainly discusses the intrinsic features of traditional ferroelectric materials, 2D ferroelectric materials, and their roles in the catalytic reaction process. The polarization characteristics of ferroelectric materials show important influence on the catalytic activities, the electron transfer, and the active centers, which could be used to boost the reaction efficiency and control the chemical reactions. Although the research of ferroelectric materials and phenomena in the chemical catalytic process is limited, great achievements and interesting findings have been made, which provide new ideas for adjusting the catalytic reaction path and controlling the selectivity. Here, we propose several possible research directions of chemical catalysis based on ferroelectric materials as in the following.

(1) Compared with traditional perovskite oxides, 2D ferroelectrics have obvious advantages, e.g., higher stabilities and larger reaction surfaces, which will have more significant effects on the catalytic process. Although a few 2D ferroelectric materials, such as In_2Se_3, $CuInP_2S_6$, and SnTe, have been experimentally

https://doi.org/10.1021/acsomega.2c06828
ACS Omega 2023, 8, 6164−6174

synthesized, more (up to 100 candidates) are theoretically predicted. Despite the promising potential as we summarized above, the quite small repository of the ferroelectric family severely limited its application in chemical catalysis. Therefore, experimental investigations on the synthesis and application of 2D ferroelectric materials in the activation of energy-related small molecules, e.g., CO_2 and O_2, are urgently required.

(2) Distinct from the common catalysts, current theoretical research shows that the polarization of ferroelectric materials can effectively control the reaction path due to the reversibility and its effects on the chemical activities. The dynamic surfaces provide an excellent platform to study the switchable chemistry. As a result, the selectivity of products will be greatly improved. Among them, 2D ferroelectric materials, which have the advantages of high stability, no surface dangling bonds, and high Curie temperature, are promising candidates to achieve high-efficiency catalysis processes. Yet, the balance between reactivity and selectivity is still an open question to be addressed, e.g., via DFT calculations.

(3) To the best of our knowledge, currently traditional DFT calculations have been mainly employed to study the catalytic reactions on the surfaces of ferroelectric materials, e.g., computing interactions energies and energy barriers. As discussed in the main paper, ferroelectric materials are often complicated systems and consist of a large number of members. As such, the DFT calculations are somewhat expensive and are almost impossible to use to predict experimentally executable systems. Therefore, the combination of DFT calculations with machine learning techniques to build up a powerful database would be an important research direction.

AUTHOR INFORMATION

Corresponding Authors

Xiao Tang − *College of Science, Nanjing Forestry University, Nanjing 210037, China*; Email: xiaotang@njfu.edu.cn

Liangzhi Kou − *School of Mechanical, Medical and Process Engineering, Queensland University of Technology, 4001 Brisbane, Australia*; orcid.org/0000-0002-3978-117X; Email: liangzhi.kou@qut.edu.au

Lei Liu − *Institute of Process Engineering, Chinese Academy of Sciences, Beijing 100049, China; Center for Computational Chemistry, College of Chemistry and Chemical Engineering, Wuhan Textile University, Wuhan 430200, China*; orcid.org/0000-0001-8850-5553; Email: liulei@wtu.edu.cn, liulei3039@gmail.com

Authors

Weitong Ding − *Institute of Process Engineering, Chinese Academy of Sciences, Beijing 100049, China*

Jing Lu − *Center for Computational Chemistry, College of Chemistry and Chemical Engineering, Wuhan Textile University, Wuhan 430200, China*

Complete contact information is available at: https://pubs.acs.org/10.1021/acsomega.2c06828

Author Contributions

⊥These authors contributed equally to the work.

Notes

The authors declare no competing financial interest.

ACKNOWLEDGMENTS

L.L. is thankful for the financial support in the form of start-up funding from Wuhan Textile University (No. 20220321).

REFERENCES

(1) Lu, H.; Wang, J.; Wang, T.; Wang, N.; Bao, Y.; Hao, H. Crystallization techniques in wastewater treatment: an overview of applications. *Chemosphere Environmental Toxicology & Risk Assessment* **2017**, *173*, 474−484.

(2) Nidheesh, P. V.; Zhou, M.; Oturan, M. A. An overview on the removal of synthetic dyes from water by electrochemical advanced oxidation processes. *Chemosphere* **2018**, *197*, 210.

(3) Wang, L.; Chen, W.; Zhang, D.; Du, Y.; Amal, R.; Qiao, S.; Wu, J.; Yin, Z. Surface strategies for catalytic CO_2 reduction: from two-dimensional materials to nanoclusters to single atoms. *Chem. Soc. Rev.* **2019**, *48*, 5310−5349.

(4) Grice, K. A. Carbon dioxide reduction with homogenous early transition metal complexes: opportunities and challenges for developing CO_2 catalysis. *Coord. Chem. Rev.* **2017**, *336*, 78−95.

(5) Faunce, T. A.; Lubitz, W.; Rutherford, A. W.; MacFarlane, D.; Moore, G. F.; Yang, P.; Nocera, D. G.; Moore, T. A.; Gregory, D. H.; Fukuzumi, S.; Yoon, K. B.; Armstrong, F. A.; Wasielewski, M. R.; Styring, S. Energy and environment policy case for a global project on artificial photosynthesis. *Energy Environ. Sci.* **2013**, *6*, 695−698.

(6) Xie, J.; Guo, C.; Yang, P.; Wang, X.; Liu, D.; Li, C. M. Bifunctional ferroelectric $BiFeO_3$ passivated $BiVO_4$ photoanode for efficient and stable solar water oxidation. *Nano Energy* **2017**, *31*, 28−36.

(7) Kakekhani, A.; Ismail-Beigi, S. Ferroelectric-based catalysis: switchable surface chemistry. *ACS Catal.* **2015**, *5*, 4537−4545.

(8) Noguera, C. Polar oxide surfaces. *J. Phys.: Condens. Matter* **2000**, *12*, R367.

(9) Watanabe, Y. Theoretical stability of the polarization in a thin semiconducting ferroelectric. *Phys. Rev. B* **1998**, *57*, 789.

(10) Radisavljevic, B.; Radenovic, A.; Brivio, J.; Giacometti, V.; Kis, A. Single-layer MoS_2 transistors. *Nat. Nanotechnol* **2011**, *6*, 147−50.

(11) Lopez-Sanchez, O.; Lembke, D.; Kayci, M.; Radenovic, A.; Kis, A. Ultrasensitive photodetectors based on monolayer MoS_2. *Nat. Nanotechnol* **2013**, *8*, 497−501.

(12) Zeng, H.; Dai, J.; Yao, W.; Xiao, D.; Cui, X. Valley polarization in MoS_2 monolayers by optical pumping. *Nat. Nanotechnol* **2012**, *7*, 490−493.

(13) Cong, C.; Shang, J.; Wu, X.; Cao, B.; Peimyoo, N.; Qiu, C.; Sun, L.; Yu, T. Synthesis and optical properties of large-area single-crystalline 2D semiconductor WS_2 monolayer from chemical vapor deposition. *Adv. Opt. Mater.* **2014**, *2*, 131−136.

(14) Bertolazzi, S.; Brivio, J.; Kis, A. Stretching and breaking of ultrathin MoS_2. *ACS Nano* **2011**, *5*, 9703−9709.

(15) Cai, Y.; Lan, J.; Zhang, G.; Zhang, Y.-W. Lattice vibrational modes and phonon thermal conductivity of monolayer MoS_2. *Phys. Rev. B* **2014**, *89*, 035438.

(16) Chhowalla, M.; Shin, H. S.; Eda, G.; Li, L. J.; Loh, K. P.; Zhang, H. The chemistry of two-dimensional layered transition metal dichalcogenide nanosheets. *Nat. Chem.* **2013**, *5*, 263−75.

(17) Lee, D.; Lu, H.; Gu, Y.; Choi, S.-Y.; Li, S.-D.; Ryu, S.; Paudel, T.; Song, K.; Mikheev, E.; Lee, S.; et al. Emergence of room-temperature ferroelectricity at reduced dimensions. *Science* **2015**, *349*, 1314−1317.

(18) Sai, N.; Kolpak, A. M.; Rappe, A. M. Ferroelectricity in ultrathin perovskite films. *Phys. Rev. B* **2005**, *72*, 020101.

(19) Wang, H.; Liu, Z.; Yoong, H.; Paudel, T. R.; Xiao, J.; Guo, R.; Lin, W.; Yang, P.; Wang, J.; Chow, G.; et al. Direct observation of room-temperature out-of-plane ferroelectricity and tunneling electroresistance at the two-dimensional limit. *Nat. Commun.* **2018**, *9*, 1−8.

https://doi.org/10.1021/acsomega.2c06828
ACS Omega 2023, 8, 6164−6174

(20) Novoselov, K. S.; Geim, A. K.; Morozov, S. V.; Jiang, D.; Zhang, Y.; Dubonos, S. V.; Grigorieva, I. V.; Firsov, A. A. Electric field effect in atomically thin carbon films. *science* **2004**, *306*, 666−669.
(21) Shirodkar, S. N.; Waghmare, U. V. Emergence of ferroelectricity at a metal-semiconductor transition in a 1 T monolayer of MoS_2. *Phys. Rev. Lett.* **2014**, *112*, 157601.
(22) Abrahams, S. Systematic prediction of new ferroelectrics on the basis of structure. *Ferroelectrics* **1990**, *104*, 37−50.
(23) Yuan, Y.; Xiao, Z.; Yang, B.; Huang, J. Arising applications of ferroelectric materials in photovoltaic devices. *J. Mater. Chem. A* **2014**, *2*, 6027−6041.
(24) Zhang, S.; Xia, R.; Shrout, T. R. Lead-free piezoelectric ceramics vs. PZT? *J. Electroceram.* **2007**, *19*, 251−257.
(25) Okuyama, M.; Ishibashi, Y. *Ferroelectric thin films: Basic properties and device physics for memory applications*; Springer Science & Business Media: Berlin/Heidelberg, Germany, 2005; Vol. *98*.
(26) Tinte, S.; Stachiotti, M.; Sepliarsky, M.; Migoni, R.; Rodriguez, C. O. Atomistic modelling of $BaTiO_3$ based on first-principles calculations. *J. Phys.: Condens. Matter* **1999**, *11*, 9679.
(27) Acosta, M.; Novak, N.; Rojas, V.; Patel, S.; Vaish, R.; Koruza, J.; Rossetti, G., Jr; Rödel, J. J. A. P. R. $BaTiO_3$-based piezoelectrics: Fundamentals, current status, and perspectives. *Applied Physics Reviews Appl. Phys. Rev.* **2017**, *4*, 041305.
(28) Buttner, R.; Maslen, E. N. Structural parameters and electron difference density in $BaTiO_3$. *Acta Crystallogr. B: Struct. Sci.* **1992**, *48*, 764−769.
(29) Kingon, A. I.; Myers, E.; Tuttle, B. Ferroelectric Thin Films II. *Materials Research Society Symposium Proceedings, Boston, MA, December 2−4, 1991*; Materials Research Society: Pittsburgh, PA, 1992; Vol. *243*.
(30) Tybell, T.; Ahn, C.; Triscone, J.-M. Ferroelectricity in thin perovskite films. *Appl. Phys. Lett.* **1999**, *75*, 856−858.
(31) Sai, N.; Kolpak, A. M.; Rappe, A. M. Ferroelectricity in ultrathin perovskite films. *Science* **2005**, *72*, 1650−1653.
(32) Gruverman, A.; Wu, D.; Lu, H.; Wang, Y.; Tsymbal, E. Y.; et al. Tunneling electroresistance effect in ferroelectric tunnel junctions at the nanoscale. *Nano Lett.* **2009**, *9*, 3539−3543.
(33) Lee, D.; Lu, H.; Gu, Y.; Choi, S. Y.; Li, S. D.; Ryu, S.; Paudel, T. R.; Song, K.; Mikheev, E.; Lee, S.; et al. Emergence of room-temperature ferroelectricity at reduced dimensions. *Science* **2015**, *349*, 1314.
(34) Cui, C.; Xue, F.; Hu, W.-J.; Li, L.-J. Two-dimensional materials with piezoelectric and ferroelectric functionalities. *npj 2D Mater. Appl.* **2018**, *2*, 1−4.
(35) Guan, Z.; Hu, H.; Shen, X.; Xiang, P.; Zhong, N.; Chu, J.; Duan, C. Recent progress in two-dimensional ferroelectric materials. *Adv. Electron. Mater.* **2020**, *6*, 1900818.
(36) Qi, L.; Ruan, S.; Zeng, Y. J. Review on recent developments in 2D ferroelectrics: theories and applications. *Adv. Mater.* **2021**, *33*, 2005098.
(37) Naguib, M.; Kurtoglu, M.; Presser, V.; Lu, J.; Niu, J.; Heon, M.; Hultman, L.; Gogotsi, Y.; Barsoum, M. W. Two-dimensional nanocrystals produced by exfoliation of Ti_3AlC_2. *Adv. Mater.* **2011**, *23*, 4248−4253.
(38) Naguib, M.; Mochalin, V. N.; Barsoum, M. W.; Gogotsi, Y. 25th anniversary article: MXenes: a new family of two-dimensional materials. *Adv. Mater.* **2014**, *26*, 992−1005.
(39) Barsoum, M. W. *MAX phases: Properties of machinable ternary carbides and nitrides*; John Wiley Sons: New York, 2013.
(40) Eklund, P.; Beckers, M.; Jansson, U.; Högberg, H.; Hultman, L. The $M_{n+X}AX_n$ phases: materials science and thin-film processing. *Thin Solid Films* **2010**, *518*, 1851−1878.
(41) Peng, Q.; Guo, J.; Zhang, Q.; Xiang, J.; Liu, B.; Zhou, A.; Liu, R.; Tian, Y. Unique lead adsorption behavior of activated hydroxyl group in two-dimensional titanium carbide. *J. Am. Chem. Soc.* **2014**, *136*, 4113−4116.
(42) Barsoum, M.; Golczewski, J.; Seifert, H.; Aldinger, F. Fabrication and electrical and thermal properties of Ti_2InC, Hf_2InC and (Ti, Hf) $_2$InC. *J. Alloys Compd.* **2002**, *340*, 173−179.
(43) El-Raghy, T.; Barsoum, M.; Sika, M. Reaction of Al with Ti_3SiC_2 in the 800−1000° C temperature range. *Mater. Sci. Eng.:A* **2001**, *298*, 174−178.
(44) Hoffman, E. N.; Yushin, G.; Barsoum, M. W.; Gogotsi, Y. Synthesis of carbide-derived carbon by chlorination of Ti_2AlC. *Chem. Mater.* **2005**, *17*, 2317−2322.
(45) Hoffman, E. N.; Yushin, G.; El-Raghy, T.; Gogotsi, Y.; Barsoum, M. W. Micro and mesoporosity of carbon derived from ternary and binary metal carbides. *Microporous Mesoporous Mater.* **2008**, *112*, 526−532.
(46) Ling, Z.; Ren, C. E.; Zhao, M.-Q.; Yang, J.; Giammarco, J. M.; Qiu, J.; Barsoum, M. W.; Gogotsi, Y. Flexible and conductive MXene films and nanocomposites with high capacitance. *Proc. Natl. Acad. Sci. U. S. A.* **2014**, *111*, 16676−16681.
(47) Naguib, M.; Mashtalir, O.; Carle, J.; Presser, V.; Lu, J.; Hultman, L.; Gogotsi, Y.; Barsoum, M. W. Two-dimensional transition metal carbides. *ACS Nano* **2012**, *6*, 1322−1331.
(48) Chandrasekaran, A.; Mishra, A.; Singh, A. K. Ferroelectricity, antiferroelectricity, and ultrathin 2D electron/hole gas in multifunctional monolayer MXene. *Nano Lett.* **2017**, *17*, 3290−3296.
(49) Zhang, L.; Tang, C.; Zhang, C.; Du, A. First-principles screening of novel ferroelectric MXene phases with a large piezoelectric response and unusual auxeticity. *Nanoscale* **2020**, *12*, 21291−21298.
(50) Fei, R.; Li, W.; Li, J.; Yang, L. Giant piezoelectricity of monolayer group IV monochalcogenides: SnSe, SnS, GeSe, and GeS. *Appl. Phys. Lett.* **2015**, *107*, 173104.
(51) Chang, K.; Küster, F.; Miller, B. J.; Ji, J. R.; Zhang, J. L.; Sessi, P.; Barraza-Lopez, S.; Parkin, S. *Microscopic manipulation of ferroelectric domains in SnSe monolayers at room temperature.* **2020**, *20*, 6590−6597.
(52) Higashitarumizu, N.; Kawamoto, H.; Lee, C. J.; Lin, B. H.; Nagashio, K.; et al. Purely in-plane ferroelectricity in monolayer SnS at room temperature. *Nat. Commun.* **2020**, *11*, 2428.
(53) Bao, Y.; Song, P.; Liu, Y.; Chen, Z.; Loh, K. P.; et al. Gate-tunable in-plane ferroelectricity in few-layer SnS. *Nano Lett.* **2019**, *19*, 5109−5117.
(54) Fei, R.; Kang, W.; Yang, L. Ferroelectricity and phase transitions in monolayer group-IV monochalcogenides. *Phys. Rev. Lett.* **2016**, *117*, 097601.
(55) Chang, K.; Liu, J.; Lin, H.; Wang, N.; Zhao, K.; Zhang, A.; Jin, F.; Zhong, Y.; Hu, X.; Duan, W. J. S.; et al. Discovery of robust in-plane ferroelectricity in atomic-thick SnTe. *Science.* **2016**, *353*, 274−278.
(56) Wan, W.; Liu, C.; Xiao, W.; Yao, Y. Promising ferroelectricity in 2D group IV tellurides: a first-principles study. *Appl. Phys. Lett.* **2017**, *111*, 132904.
(57) Zhang, X.; Yang, Z.; Chen, Y. Novel two-dimensional ferroelectric PbTe under tension: a first-principles prediction. *J. Appl. Phys.* **2017**, *122*, 064101.
(58) Wu, M.; Zeng, X. C. Intrinsic ferroelasticity and/or multiferroicity in two-dimensional phosphorene and phosphorene analogues. *Nano Lett.* **2016**, *16*, 3236−41.
(59) Abrahams, S. C. Systematic prediction of new ferroelectrics on the basis of structure. *Ferroelectrics* **1990**, *104*, 37−50.
(60) Cui, C.; Hu, W. J.; Yan, X.; Addiego, C.; Gao, W.; Wang, Y.; Wang, Z.; Li, L.; Cheng, Y.; Li, P.; Zhang, X.; Alshareef, H. N.; Wu, T.; Zhu, W.; Pan, X.; Li, L. J. Intercorrelated in-plane and out-of-plane ferroelectricity in ultrathin two-dimensional layered semiconductor In_2Se_3. *Nano Lett.* **2018**, *18*, 1253−1258.
(61) Ding, W.; Zhu, J.; Wang, Z.; Gao, Y.; Xiao, D.; Gu, Y.; Zhang, Z.; Zhu, W. Prediction of intrinsic two-dimensional ferroelectrics in In_2Se_3 and other III2-VI3 van der Waals materials. *Nat. Commun.* **2017**, *8*, 14956.
(62) Zhou, Y.; Wu, D.; Zhu, Y.; Cho, Y.; He, Q.; Yang, X.; Herrera, K.; Chu, Z.; Han, Y.; Downer, M. C.; Peng, H.; Lai, K. Out-of-plane piezoelectricity and ferroelectricity in layered alpha-In_2Se_3 nanoflakes. *Nano Lett.* **2017**, *17*, 5508−5513.

https://doi.org/10.1021/acsomega.2c06828
ACS Omega 2023, 8, 6164−6174

(63) Xiao, J.; Zhu, H.; Wang, Y.; Feng, W.; Hu, Y.; Dasgupta, A.; Han, Y.; Wang, Y.; Muller, D. A.; Martin, L. W.; Hu, P.; Zhang, X. Intrinsic two-dimensional ferroelectricity with dipole locking. *Phys. Rev. Lett.* **2018**, *120*, 227601.
(64) Novoselov, K. S.; Jiang, D.; Schedin, F.; Booth, T.; Khotkevich, V.; Morozov, S.; Geim, A. K. Two-dimensional atomic crystals. *Proc. Natl. Acad. Sci. U. S. A.* **2005**, *102*, 10451−10453.
(65) Duerloo, K.-A. N.; Ong, M. T.; Reed, E. J. Intrinsic piezoelectricity in two-dimensional materials. *J. Phys. Chem. Lett.* **2012**, *3*, 2871−2876.
(66) Zhu, H.; Wang, Y.; Xiao, J.; Liu, M.; Xiong, S.; Wong, Z. J.; Ye, Z.; Ye, Y.; Yin, X.; Zhang, X. Observation of piezoelectricity in free-standing monolayer MoS_2. *Nat. Nanotechnol.* **2015**, *10*, 151−5.
(67) Mak, K. F.; Lee, C.; Hone, J.; Shan, J.; Heinz, T. F. Atomically thin MoS_2: a new direct-gap semiconductor. *Phys. Rev. Lett.* **2010**, *105*, 136805.
(68) Shirodkar, S. N.; Waghmare, U. V. Emergence of ferroelectricity at a metal-semiconductor transition in a 1T monolayer of MoS_2. *Phys. Rev. Lett.* **2014**, *112*, 157601.
(69) Fei, Z.; Zhao, W.; Palomaki, T. A.; Sun, B.; Miller, M. K.; Zhao, Z.; Yan, J.; Xu, X.; Cobden, D. H. Ferroelectric switching of a two-dimensional metal. *Nature* **2018**, *560*, 336−339.
(70) Barua, M.; Ayyub, M. M.; Vishnoi, P.; Pramoda, K.; Rao, C. Photochemical HER activity of layered metal phospho-sulfides and-selenides. *J. Mater. Chem. A* **2019**, *7*, 22500−22506.
(71) Anantharaj, S.; Ede, S. R.; Sakthikumar, K.; Karthick, K.; Mishra, S.; Kundu, S. Recent trends and perspectives in electrochemical water splitting with an emphasis on sulfide, selenide, and phosphide catalysts of Fe, Co, and Ni: a review. *ACS Catal.* **2016**, *6*, 8069−8097.
(72) Lin, B.; Chaturvedi, A.; Di, J.; You, L.; Lai, C.; Duan, R.; Zhou, J.; Xu, B.; Chen, Z.; Song, P.; Peng, J.; Ma, B.; Liu, H.; Meng, P.; Yang, G.; Zhang, H.; Liu, Z.; Liu, F. Ferroelectric-field accelerated charge transfer in 2D $CuInP_2S_6$ heterostructure for enhanced photocatalytic H_2 evolution. *Nano Energy* **2020**, *76*, 104972.
(73) Simon, A.; Ravez, J.; Maisonneuve, V.; Payen, C.; Cajipe, V. Paraelectric-ferroelectric transition in the lamellar thiophosphate $CuInP_2S_6$. *Chem. Mater.* **1994**, *6*, 1575−1580.
(74) Belianinov, A.; He, Q.; Dziaugys, A.; Maksymovych, P.; Eliseev, E.; Borisevich, A.; Morozovska, A.; Banys, J.; Vysochanskii, Y.; Kalinin, S. V. $CuInP_2S_6$ Room Temperature Layered Ferroelectric. *Nano Lett.* **2015**, *15*, 3808.
(75) Liu, F.; You, L.; Seyler, K. L.; Li, X.; Yu, P.; Lin, J.; Wang, X.; Zhou, J.; Wang, H.; He, H.; Pantelides, S. T.; Zhou, W.; Sharma, P.; Xu, X.; Ajayan, P. M.; Wang, J.; Liu, Z. Room-temperature ferroelectricity in $CuInP_2S_6$ ultrathin flakes. *Nat. Commun.* **2016**, *7*, 12357.
(76) Maisonneuve, V.; Cajipe, V. B.; Simon, A.; Von der Muhll, R.; Ravez, J. Ferrielectric ordering in lamellar $CuInP_2S_6$. *Phys. Rev. B* **1997**, *56*, 10860.
(77) Adachi, M.; Akishige, Y.; Asahi, T.; Deguchi, K.; Gesi, K.; Hasebe, K.; Hikita, T.; Ikeda, T.; Iwata, Y.; et al. *Ferroelectrics and related substances: Oxides*; Landolt-Bornstein, New Series, Group III; Springer-Verlag: Berlin/Heidelberg, Germany, 2001; Vol. *36*.
(78) Xu, B.; Xiang, H.; Xia, Y.; Jiang, K.; Wan, X.; He, J.; Yin, J.; Liu, Z. Monolayer $AgBiP_2Se_6$: an atomically thin ferroelectric semiconductor with out-plane polarization. *Nanoscale* **2017**, *9*, 8427−8434.
(79) Yun, Y.; Altman, E. I. Using ferroelectric poling to change adsorption on oxide surfaces. *J. Am. Chem. Soc.* **2007**, *129*, 15684−15689.
(80) Parravano, G. Ferroelectric transitions and heterogenous catalysis. *J. Chem. Phys.* **1952**, *20*, 342−343.
(81) Ramos-Moore, E.; Baier-Saip, J.; Cabrera, A. L. Desorption of carbon dioxide from small potassium niobate particles induced by the particles' ferroelectric transition. *Surf. Sci.* **2006**, *600*, 3472−3476.
(82) Yun, Y.; Kampschulte, L.; Li, M.; Liao, D.; Altman, E. I. Effect of ferroelectric poling on the adsorption of 2-propanol on $LiNbO_3$(0001). *J. Phys. Chem. C* **2007**, *111*, 13951−13956.
(83) Zhao, M. H.; Bonnell, D. A.; Vohs, J. M. Effect of ferroelectric polarization on the adsorption and reaction of ethanol on $BaTiO_3$. *Surf. Sci.* **2008**, *602*, 2849−2855.
(84) Kolpak, A. M.; Grinberg, I.; Rappe, A. M. Polarization effects on the surface chemistry of $PbTiO_3$-supported Pt films. *Phys. Rev. Lett.* **2007**, *98*, 166101.
(85) Kakekhani, A.; Ismail-Beigi, S. Polarization-driven catalysis via ferroelectric oxide surfaces. *Phys. Chem. Chem. Phys.* **2016**, *18*, 19676−95.
(86) Kakekhani, A.; Ismail-Beigi, S.; Altman, E. I. Ferroelectrics: a pathway to switchable surface chemistry and catalysis. Altman, E. I. *Surf. Sci.* **2016**, *650*, 302−316.
(87) Kakekhani, A.; Ismail-Beigi, S. Ferroelectric oxide surface chemistry: water splitting via pyroelectricity. *J. Mater. Chem. A* **2016**, *4*, 5235−5246.
(88) Tang, X.; Shang, J.; Ma, Y.; Gu, Y.; Chen, C.; Kou, L. Tuning magnetism of metal porphyrazine molecules by a ferroelectric In_2Se_3 monolayer. *ACS Appl. Mater. Interfaces* **2020**, *12*, 39561−39566.
(89) Tang, X.; Shang, J.; Gu, Y.; Du, A.; Kou, L. Reversible gas capture using a ferroelectric switch and 2D molecule multiferroics on the In_2Se_3 monolayer. *J. Mater. Chem. A* **2020**, *8*, 7331−7338.
(90) Wan, T. L.; Shang, J.; Gu, Y.; Kou, L. Ferroelectric controlled gas adsorption in doped graphene/In_2Se_3 heterostructure. *Adv. Mater. Technol.* **2022**, *7*, 2100463.
(91) Kudo, A.; Miseki, Y. Heterogeneous photocatalyst materials for water splitting. *Chem. Soc. Rev.* **2009**, *38*, 253−278.
(92) Li, L.; Salvador, P. A.; Rohrer, G. S. Photocatalysts with internal electric fields. *Nanoscale* **2014**, *6*, 24−42.
(93) Inoue, Y.; Hayashi, O.; Sato, K. Faraday transactions photocatalytic activities of potassium-doped lead niobates and the effect of poling. *J. Chem. Soc., Faraday Trans.* **1990**, *86*, 2277−2282.
(94) Wang, P.; Liu, H.; Zong, Y.; Wen, H.; Xia, J. B.; Wu, H. B. Two-dimensional In_2X_2X' (X and X' = S, Se, and Te) monolayers with an intrinsic electric field for high-performance photocatalytic and piezoelectric applications. *ACS Appl. Mater. Interfaces* **2021**, *13*, 34178−34187.
(95) Jin, S.; Hao, Z.; Zhang, K.; Yan, Z.; Chen, J. Advances and challenges for the electrochemical reduction of CO_2 to CO: from fundamentals to industrialization. *Angew. Chem., Int. Ed.* **2021**, *133*, 20795.
(96) Giocondi, J. L.; Rohrer, G. S. Spatial separation of photochemical oxidation and reduction reactions on the surface of ferroelectric $BaTiO_3$. *J. Phys. Chem. B* **2001**, *105*, 8275−8277.
(97) Bhardwaj, A.; Burbure, N. V.; Gamalski, A.; Rohrer, G. S. Composition dependence of the photochemical reduction of Ag by $Ba_{1-x}Sr_xTiO_3$. *Chem. Mater.* **2010**, *22*, 3527−3534.
(98) Schultz, A. M.; Zhang, Y.; Salvador, P. A.; Rohrer, G. S. Effect of crystal and domain orientation on the visible-light photochemical reduction of Ag on $BiFeO_3$. *ACS Appl. Mater. Interfaces* **2011**, *3*, 1562−1567.
(99) Wu, Q.; Ma, Y.; Wang, H.; Zhang, S.; Huang, B.; Dai, Y. Trifunctional electrocatalysts with high efficiency for the oxygen reduction reaction, oxygen evolution reaction, and Na-O_2 battery in heteroatom-doped janus monolayer MoSSe. *ACS Appl. Mater. Interfaces* **2020**, *12*, 24066−24073.
(100) Kushwaha, H.; Halder, A.; Vaish, R. Ferroelectric electrocatalysts: a new class of materials for oxygen evolution reaction with synergistic effect of ferroelectric polarization. *J. Mater. Sci.* **2018**, *53*, 1414−1423.
(101) Li, X.; Sun, Y.; Wu, Q.; Liu, H.; Gu, W.; Wang, X.; Cheng, Z.; Fu, Z.; Lu, Y. Optimized electronic configuration to improve the surface absorption and bulk conductivity for enhanced oxygen evolution reaction. *J. Am. Chem. Soc.* **2019**, *141*, 3121−3128.
(102) Li, X.; Liu, H.; Chen, Z.; Wu, Q.; Yu, Z.; Yang, M.; Wang, X.; Cheng, Z.; Fu, Z.; Lu, Y. Enhancing oxygen evolution efficiency of multiferroic oxides by spintronic and ferroelectric polarization regulation. *Nat. Commun.* **2019**, *10*, 1409.
(103) Kim, H. S. Computational design of a switchable heterostructure electrocatalyst based on a two-dimensional ferro-

https://doi.org/10.1021/acsomega.2c06828
ACS Omega 2023, 8, 6164−6174

electric In_2Se_3 material for the hydrogen evolution reaction. *J. Mater. Chem. A* **2021**, *9*, 11553−11562.
(104) Hu, T.; Su, H.; Li, Q.; Kan, E. Tunable ferroelectric single-atom catalysis of CO oxidation using a Pt/In_2Se_3 monolayer. *J. Mater. Chem. A* **2020**, *8*, 20725−20731.
(105) Ju, L.; Tan, X.; Mao, X.; Gu, Y.; Smith, S.; Du, A.; Chen, Z.; Chen, C.; Kou, L. Controllable CO_2 electrocatalytic reduction via ferroelectric switching on single atom anchored In_2Se_3 monolayer. *Nat. Commun.* **2021**, *12*, 5128.

https://doi.org/10.1021/acsomega.2c06828
ACS Omega 2023, 8, 6164−6174